AGU PUBLICATIONS

Geophysical Research Letters

Supporting Information for

Disentangling the mechanisms of ENSO response to tropical volcanic eruptions

Francesco S.R. Pausata[1*], Yang Zhao[2], Davide Zanchettin[3], Rodrigo Caballero[4] and David S. Battisti[5,6]

[1]Centre ESCER (Étude et la Simulation du Climat à l'Échelle Régionale) and GEOTOP (Research Center on the dynamics of the Earth System), Department of Earth and Atmospheric Sciences, University of Quebec in Montreal, Montreal, QC H3C 3J7, Canada

[2] State Key Laboratory of Severe Weather, Chinese Academy of Meteorological Sciences, Beijing, China

[3]Department of Environmental Sciences, Informatics and Statistics, University Ca'Foscari of Venice, Mestre, Italy

[4]Department of Meteorology, Stockholm University and Bolin Centre for Climate Research, Stockholm, Sweden,

[5]Department of Atmospheric Sciences, University of Washington, Seattle, Washington, USA

[6]UNI Research, Bergen, Norway

*Corresponding author: Francesco S.R. Pausata (pausata.francesco@uqam.ca)

Contents of this file

Figures S1 to S8

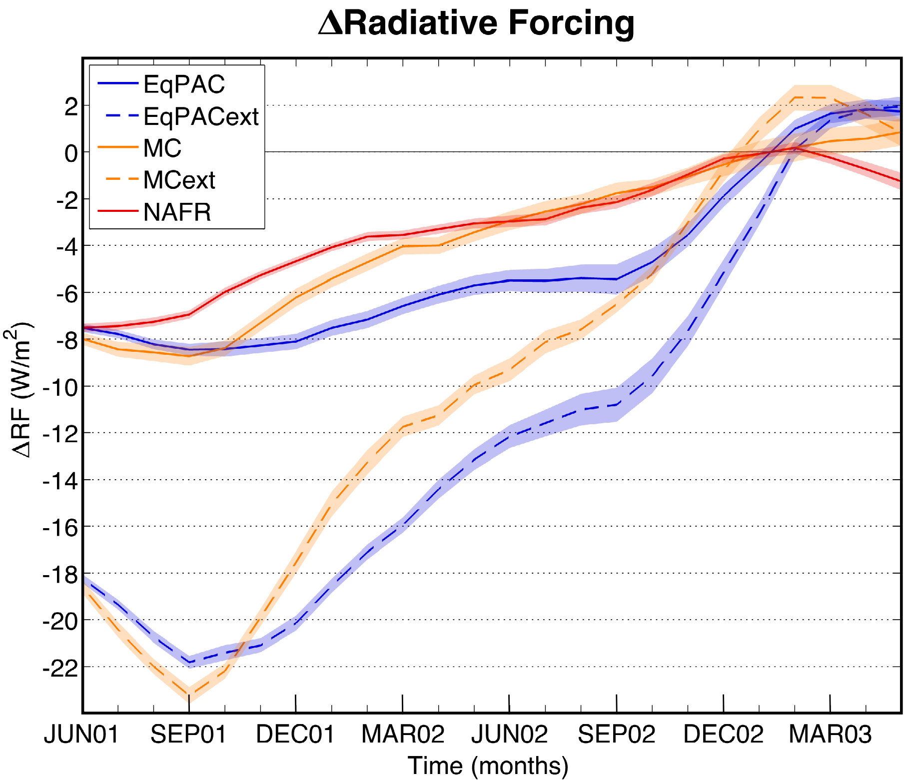

Figure S1. Radiative forcing. Changes in the net radiative forcing at the top of the atmosphere for each ensemble experiment relative to the no-volcano case. Shading represents twice the standard error of the mean (approximate 95% confidence intervals).

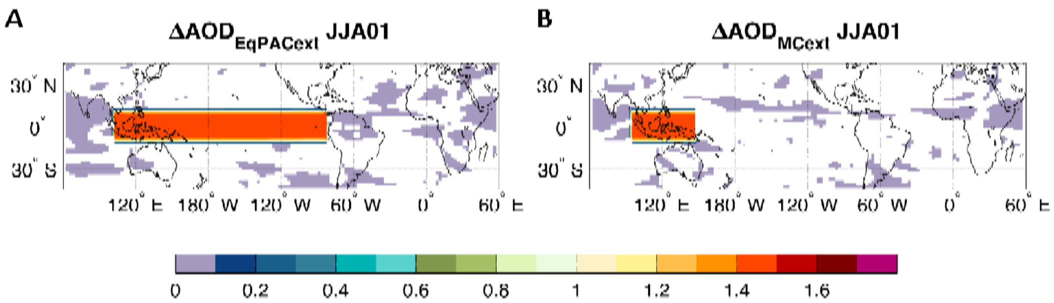

Figure S2. Volcanic forcing in extreme experiments. Anomalies in aerosol optical depth (at 550 nm) in the extreme Maritime Continent – MC experiment (A) and the extreme Equatorial Pacific – EqPAC experiment (B) for the summer (June to August – JJA) following the imposed changes in AOD relative to the no-volcano simulations.

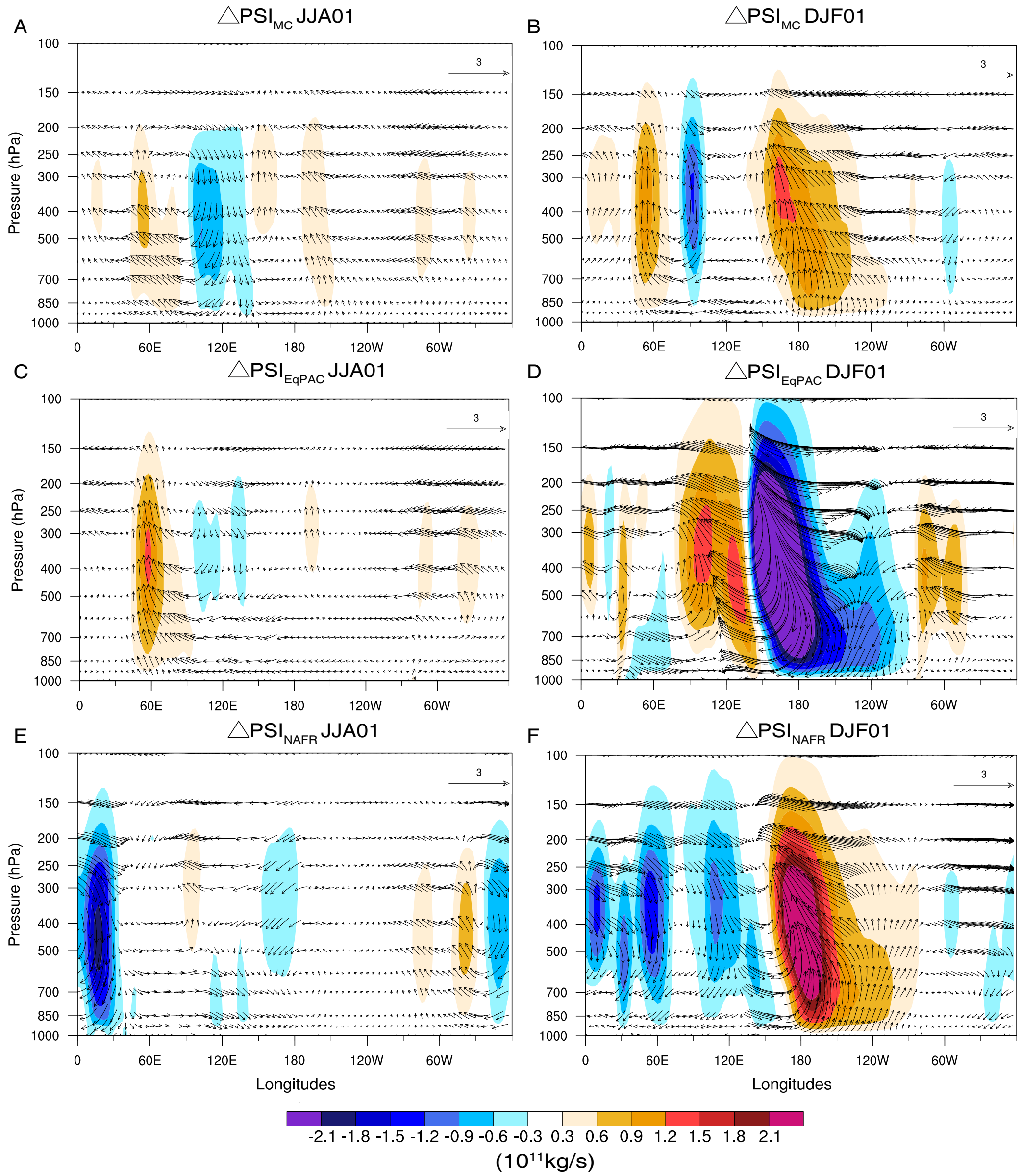

Figure S3. Walker Circulation response in the first post-eruption year. Changes in the zonal stream function (10^{11} kg/s) and vertical winds (m/s) averaged over the Equatorial Pacific (5°S – 5°N) for the first summer (June to August – JJA; left) and winter (December to February – DJF; right) following the AOD imposed anomalies above the Maritime Continent – MC (A - B), the equatorial Pacific – EqPAC (C – D) and the tropical and northern Africa – NAFR (E – F) relative to the no-volcano simulations.

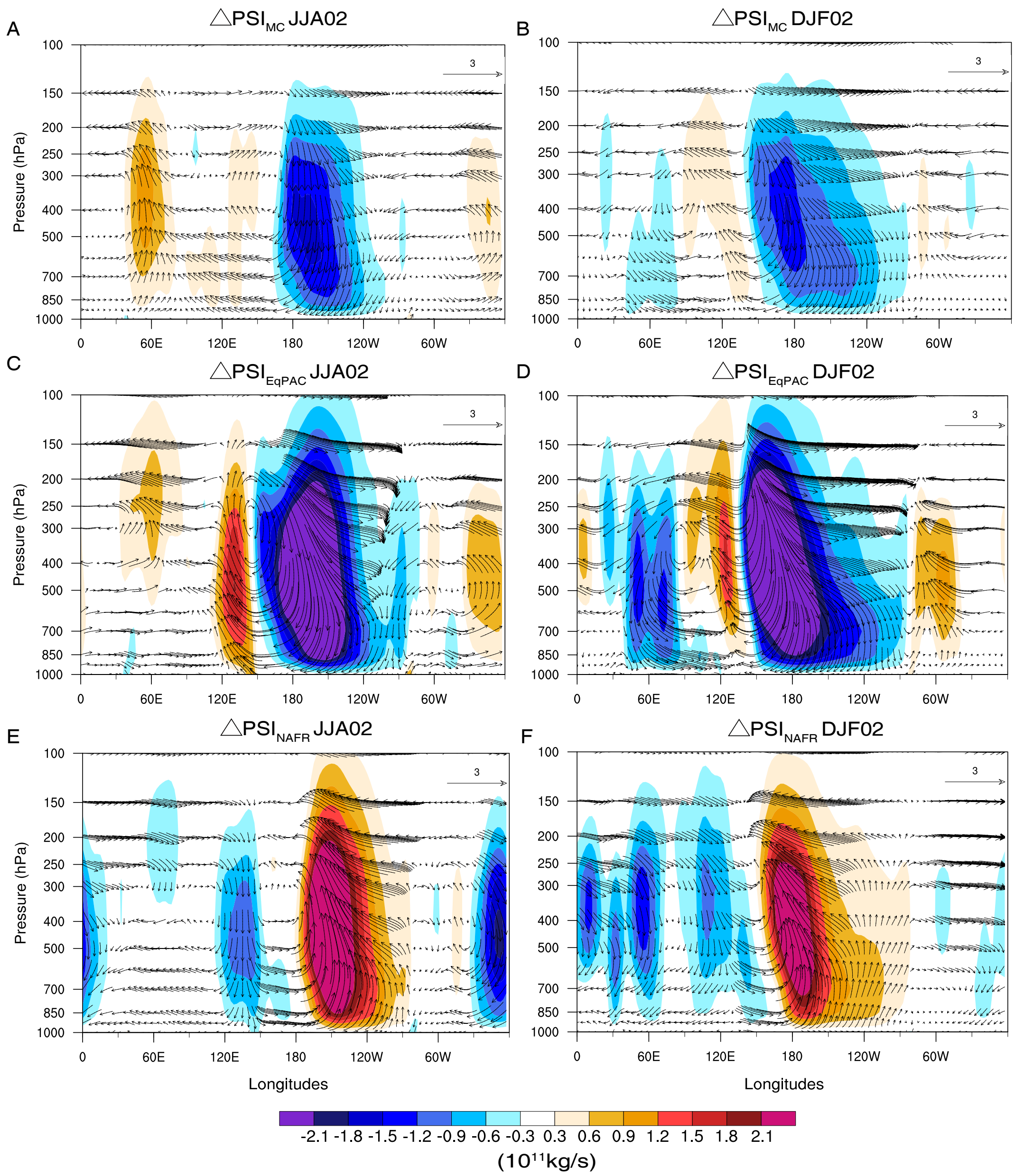

Figure S4. Walker Circulation response in the second post-eruption year. Changes in the zonal stream function (10^{11} kg/s) and vertical winds (m/s) averaged over the Equatorial Pacific (5°S – 5°N) for the second summer (June to August – JJA; left) and winter (December to February – DJF; right) following the AOD imposed anomalies above the Maritime Continent – MC (A and B), the equatorial Pacific – EqPAC (C and D) and the tropical and northern Africa – NAFR (E and F) relative to the no-volcano simulations.

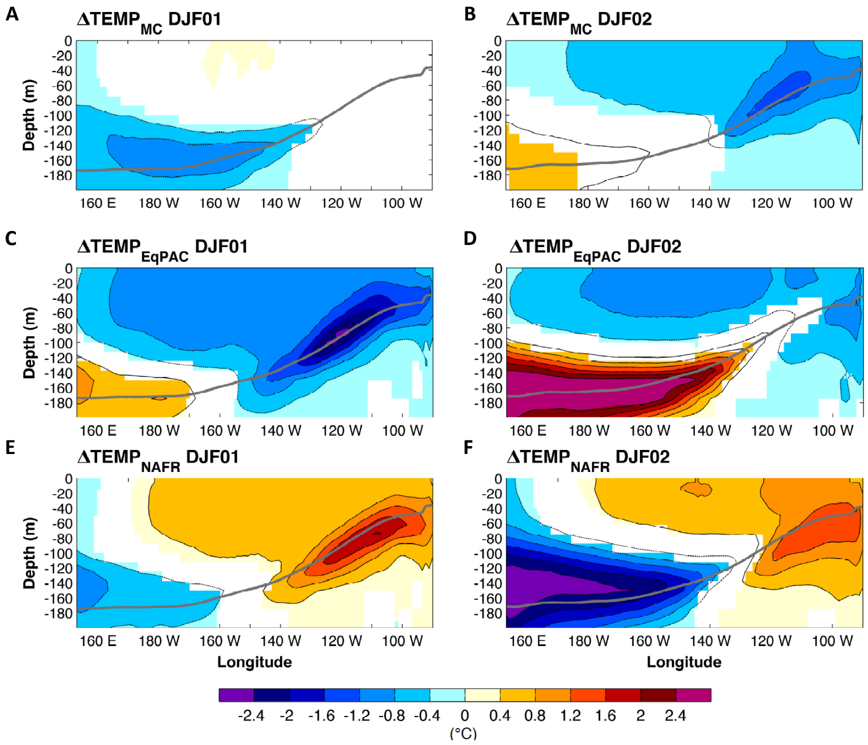

Figure S5. Thermocline response in the first and second post-eruption winter. Ocean temperature (°C) anomalies in the Equatorial Pacific (5°S – 5°N) for the first (left) and second (right) winter (December to February – DJF) following the AOD imposed anomalies over the Maritime Continent – MC (A and B), the equatorial Pacific – EqPAC (C and D) and the tropical and northern Africa – NAFR (E and F) relative to the no-volcano simulations. Only values that are significantly different at the 5% level using a *t* test are shaded. The contours follow the color bar intervals (solid for positive and dashed for negative anomalies; the zero line is omitted). The bold grey line shows the climatological thermocline depth for the no-volcano members (as defined using the 20°C isotherm).

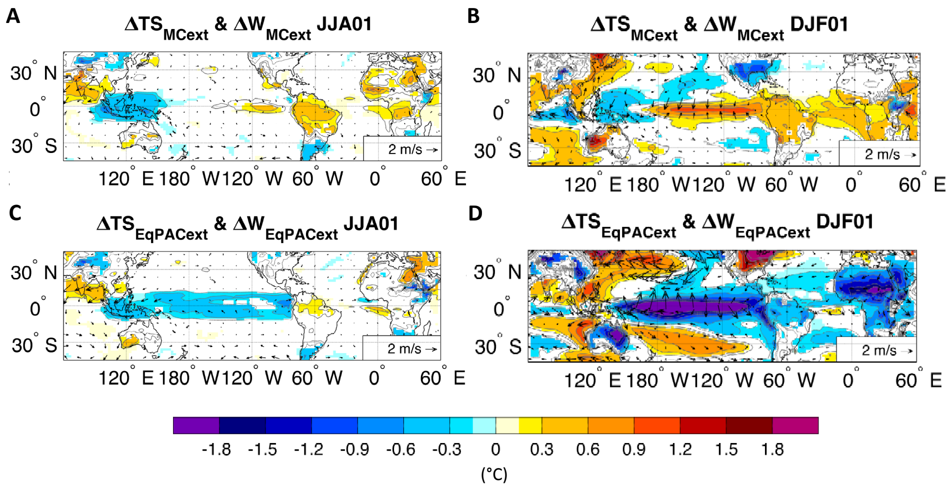

Figure S6. Surface air temperature and wind response for the extreme experiments. Changes in surface temperature (°C, contours and shadings) and wind (m/s, arrows) in the summer (June to August – JJA; left) and winter (December to February – DJF; right) following the AOD imposed anomalies for extreme experiments (MC extreme – A and B; and EqPAC extreme – C and D) relative to the no-volcano case. Only temperature values that are significantly different at the 5% level using a local (grid-point) *t* test are shaded. The contours follow the colorbar intervals (solid for positive and dashed for negative anomalies; the zero line is omitted).

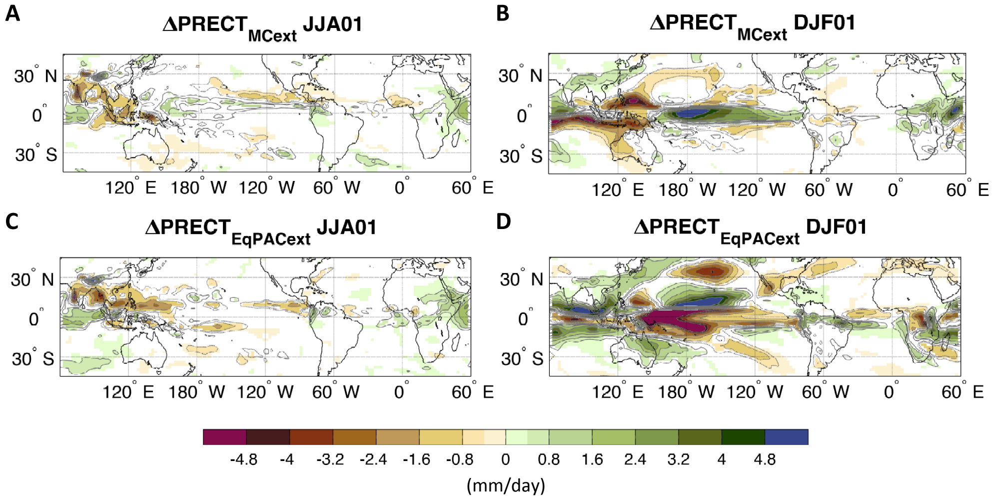

Figure S7. Rainfall response for the extreme experiments. Changes in precipitation (mm/day, contours and shadings) in the summer (June to August – JJA) and winter (December to February – DJF) following the AOD imposed anomalies for extreme experiments (MC extreme – A and B; and EqPAC extreme – C and D) relative to the no-volcano case. Only temperature values that are significantly different at the 5% level using a local (grid-point) *t* test are shaded. The contours follow the colorbar intervals (solid for positive and dashed for negative anomalies; the zero line is omitted).

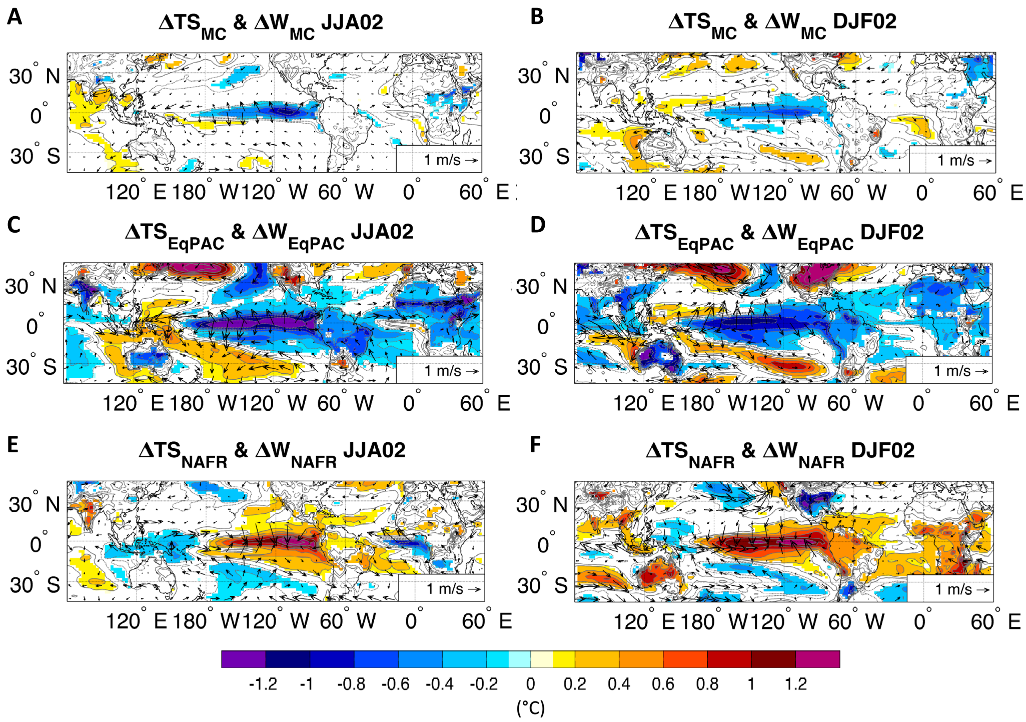

Figure S8. Surface air temperature and wind response in the second post-eruption year. Changes in surface temperature (°C, contours and shadings) and wind (m/s, arrows) in the summer (June to August – JJA) and winter (December to February – DJF) following the AOD imposed anomalies above the Maritime Continent – MC (A and B), the equatorial Pacific – EqPAC (C and D) and the tropical and northern Africa – NAFR (E and F). Only temperature values that are significantly different at the 5% level using a local (grid-point) *t* test are shaded. The contours follow the colorbar intervals (solid for positive and dashed for negative anomalies; the zero line is omitted).